

# KINEMATICS OF A TRANSLATION-ROTATION HYBRID PARALLEL ROBOT

ȘTEFAN STAIUCU

*Abstract.* Matrix relations for kinematics analysis of a spatial two-module hybrid parallel mechanism are established in this paper. Knowing the relative motions of the moving platforms, the inverse kinematics problem is solved based on a set of connectivity relations. Finally, compact results and graphs of simulation for the input relative displacements, velocities and accelerations are obtained.

*Key words:* connectivity relations, hybrid parallel robot, kinematics.

## LIST OF SYMBOLS

$\vec{u}_1, \vec{u}_2, \vec{u}_3$	three orthogonal unit vectors
$P_{\tau, \tau-1}, Q_{\tau, \tau-1}$	relative orthogonal matrices of transformation
$\alpha_i, \alpha_j$	angles giving the position of universal joints
$\beta_\sigma$	initial inclination of legs
$\lambda_{32}^i$	relative displacement of $T_3^i$ link
$\Phi_{\tau, \tau-1}^i$	relative rotation angle of $T_\tau^i$ rigid body
$\vec{\omega}_{\tau, \tau-1}^i$	relative angular velocity of $T_\tau^i$
$\vec{\omega}_{\tau 0}^i$	absolute angular velocity of $T_\tau^i$
$\tilde{\omega}_{\tau, \tau-1}^i$	skew symmetric matrix associated to the vector $\vec{\omega}_{\tau, \tau-1}^i$
$\vec{\varepsilon}_{\tau, \tau-1}^i$	relative angular acceleration of $T_\tau^i$
$\vec{\varepsilon}_{\tau 0}^i$	absolute angular acceleration of $T_\tau^i$
$\tilde{\varepsilon}_{\tau, \tau-1}^i$	skew symmetric matrix associated to the vector $\vec{\varepsilon}_{\tau, \tau-1}^i$
$\vec{r}_{k, k-1}^A$ ( $k = 1, 2, 3$ )	relative position vector of the centre of $A_k$ joint
$\vec{v}_{k, k-1}^A$	relative velocity of the centre $A_k$
$\vec{\gamma}_{k, k-1}^A$	relative acceleration of the centre $A_k$

---

“Politehnica” University of Bucharest, Department of Mechanics, Romania

Ro. J. Techn. Sci. – Appl. Mechanics, Vol. 60, N<sup>os</sup> 3, pp. 171–183, Bucharest, 2015

## 1. INTRODUCTION

Compared with serial robots, the parallel robots have specific characteristics: higher structural rigidity, better orientation accuracy, stable functioning, larger dynamic charge capacity and suitable position of the actuating systems. Provided with closed-loop structures, the links of parallel robots can be connected by spherical joints, universal joints, revolute joints or prismatic joints [1, 2]. Typically, the number of actuators is equal to the number of degrees of freedom such that every link is controlled at or near its base [3, 4].

A hybrid manipulator is a combination of closed-chain and open-chain planar and spatial mechanisms or a sequence of parallel robots [5–8]. A serial-parallel manipulator has several modules with parallel structure that are connected serially [9]. Shahinpoor [10] obtained and solved numerically a system of nonlinear equations for the inverse kinematics problem of a hybrid robotic system consisting of two serially connected parallel manipulators. Cheng *et al.* [11] used a numerical Newton-Raphson method to obtain the solution of the direct kinematics problem of a 10-DOF hybrid redundant manipulator, containing a closed-loop slider-crank mechanism and a parallel-driven mechanism.

Based on screw theory, Gallardo *et al.* [12] addressed a complete kinematics analysis of a modular spatial hyper-redundant manipulator built with a variable number of serially connected mechanical modules.

Recursive method based on several connectivity relations is applied in the present paper to the analysis of a spatial two-module hybrid manipulator, reducing together the number of equations and computation operations significantly by using a set of matrices for kinematics modelling. Considering the lower module as a positional mechanism and the upper module as an orientation device, we analyze the geometry, the position and the kinematics of a hybrid manipulator composed of serially connected two different parallel robots, each mechanism having three degrees of freedom.

## 2. GEOMETRICAL ARCHITECTURE

Having six degrees of freedom, the hybrid robot here analyzed is made up of two different 3-DOF parallel modules, which are serially connected to a fixed base, but the study can be easily extended to a complex robotic system composed of a multitude connected parallel robots. Practically, the degrees-of-freedom value  $F = 6$  of the hybrid mechanism is equal to the degrees of freedom associated with all the moving links  $\nu = 24$  minus the total number of independent constraint relations  $l = 18$  imposed by the joints.

The structure of the lower parallel module, for example, consists of a fixed circular base  $A_1B_1C_1$  of radius  $R_1$  represented by three universal joints located at

the points  $A_1, B_1, C_1$ , a circular mobile platform  $A_4B_4C_4$  of radius  $r_1$  and three extensible legs with identical kinematical structure. Each limb connects the fixed base to the moving platform by two universal ( $U$ ) joints interconnected through a prismatic ( $P$ ) joint made up of a cylinder and a piston.

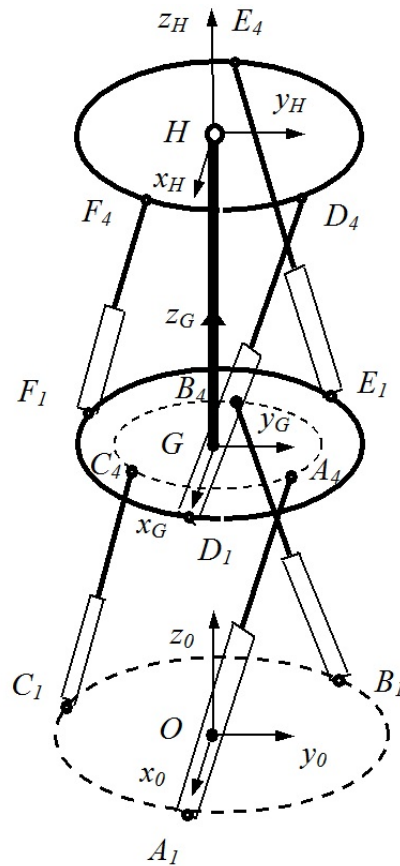


Fig. 1 – Hybrid parallel robot.

Hydraulic or pneumatic systems, but also electrical prismatic actuators with very good dynamic behaviour and positioning accuracy, can be used to vary the lengths of the prismatic joints and to control the location of the platform. Since each  $U$  joint consists of two intersecting revolute ( $R$ ) joints, each leg is equivalent to a  $RRPRR$  kinematical chain. But, the mechanism can be arranged to achieve only translational motions with certain conditions satisfied, i.e., in each kinematical chain the axis of the first revolute joint is parallel to that of the last one and the two intermediate joint axes are parallel to one another. Thus, the first parallel module has three active mobile prismatic joints and six passive universal joints.

The architecture of the upper parallel module consists of a new circular mobile platform  $D_4E_4F_4$  of radius  $r_2$  connected first to the moving base through a central spherical joint  $H$  and three identical extensible  $UPS$  legs, each comprising a prismatic actuator made up of a cylinder and a piston. The upper end of each leg is connected to the moving platform by a spherical joint, whereas the lower end is connected to the first moving platform by a universal joint situated on a circle of radius  $R_2$ . We note that this spatial mechanism, sometimes, is not considered a spherical mechanism, because the three legs and the moving platform do not have a common stationary point.

The moving platforms are initially considered both at a *central configuration*, where are not rotated with respect to the fixed frame and their centers are located at given relative elevations  $OG = h_1$ ,  $GH = h_2$  above the fixed base. We assign a fixed Cartesian coordinate system  $Ox_0y_0z_0$  at the point  $O$  of the fixed frame and also two mobile frames  $Gx_Gy_Gz_G$  and  $Hx_Hy_Hz_H$  on the moving platforms at their mass centers  $G$  and  $H$ , respectively (Fig. 1).

Since the hybrid manipulator is an assembly of links and joints, this can be symbolised in a more abstract form known as equivalent graph representation, using the associated graph to represent the topology of the mechanism. In the kinematical graph representation, with *six independent loops*, the links are denoted by vertices, the prismatic joints by thick edges, the revolute and spherical joints by thin edges and, finally, the fixed link 0 by two small concentric circles (Fig. 2).

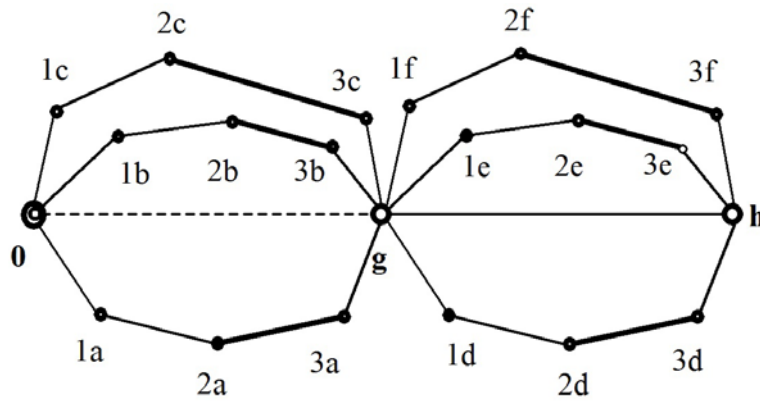


Fig. 2 – Associated graph of the mechanism.

The active leg  $A$  of the lower module (Fig. 3), for example, consists of a little cross of a fixed Hooke universal joint linked at the frame  $A_1x_1^Ay_1^Az_1^A$ , characterised by the angle of rotation  $\varphi_{10}^A$ , the angular velocity  $\omega_{10}^A = \dot{\varphi}_{10}^A$  and the angular acceleration  $\varepsilon_{10}^A = \dot{\omega}_{10}^A$ , connected at a moving cylinder  $A_2x_2^Ay_2^Az_2^A$  of length  $l_2$ ,

having a relative rotation around  $A_2 z_2^A$  axis with the angle  $\varphi_{21}^A$ , so that  $\omega_{21}^A = \dot{\varphi}_{21}^A$ ,  $\varepsilon_{21}^A = \dot{\omega}_{21}^A$ . An actuated prismatic joint is as well as a piston of length  $A_3 A_4 = l_3$  linked to  $A_3 x_3^A y_3^A z_3^A$  frame, which has the relative displacement  $\lambda_{32}^A$ , the velocity  $v_{32}^A = \dot{\lambda}_{32}^A$  and the acceleration  $\gamma_{32}^A = \ddot{\lambda}_{32}^A$ . Finally, a second universal joint  $A_4$  is attached at the edge of circular moving platform. We also consider that the three sliders are initially starting from the same position  $l_1 = h_1 / \sin \beta_1 - l_3$  and that the angles of orientation of universal joints are given by

$$\alpha_A = 0, \quad \alpha_B = -\alpha_C = \frac{2\pi}{3}, \quad v_1 = \frac{\pi}{6}, \quad (1)$$

$$(R_1 - r_1 \cos v_1) \tan \delta_1 = r_1 \sin v_1, \quad r_1 \sin v_1 \tan \beta_1 = h_1 \sin \delta_1,$$

where the angle  $v_1$  is defined as *twist* angle of the parallel robot and  $\delta_1, \beta_1$  are two constant angles of rotation around the axes  $z_1^A$  and  $z_2^A$ , respectively.

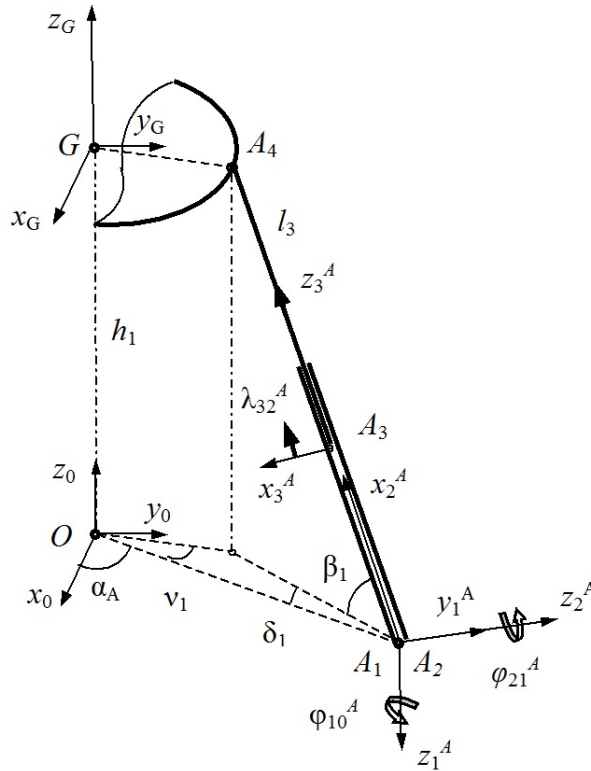


Fig. 3 – Kinematical scheme of first leg A of lower module.

One of identical legs of upper module (leg  $D_1D_2D_3D_4$ , for example, Fig. 4) consists of a universal joint linked at the frame  $D_1x_1^D y_1^D z_1^D$ , which has the angular velocity  $\omega_{10}^D = \dot{\varphi}_{10}^D$ , the angular acceleration  $\varepsilon_{10}^D = \dot{\omega}_{10}^D$  and is connected at a moving cylinder  $D_2x_2^D y_2^D z_2^D$ , having a relative rotation about  $D_2z_2^D$  axis with the angle  $\varphi_{21}^D$ , so that  $\omega_{21}^D = \dot{\varphi}_{21}^D$ ,  $\varepsilon_{21}^D = \dot{\omega}_{21}^D$ . A new actuated prismatic joint is, also, as well as a piston  $D_3D_4 = l_6$  linked to  $D_3x_3^D y_3^D z_3^D$  frame, having a relative displacement  $\lambda_{32}^D$ , velocity  $v_{32}^D = \dot{\lambda}_{32}^D$  and acceleration  $\gamma_{32}^D = \dot{v}_{32}^D$ . Finally, a ball-joint  $D_4$  is introduced at the edge of second moving platform.

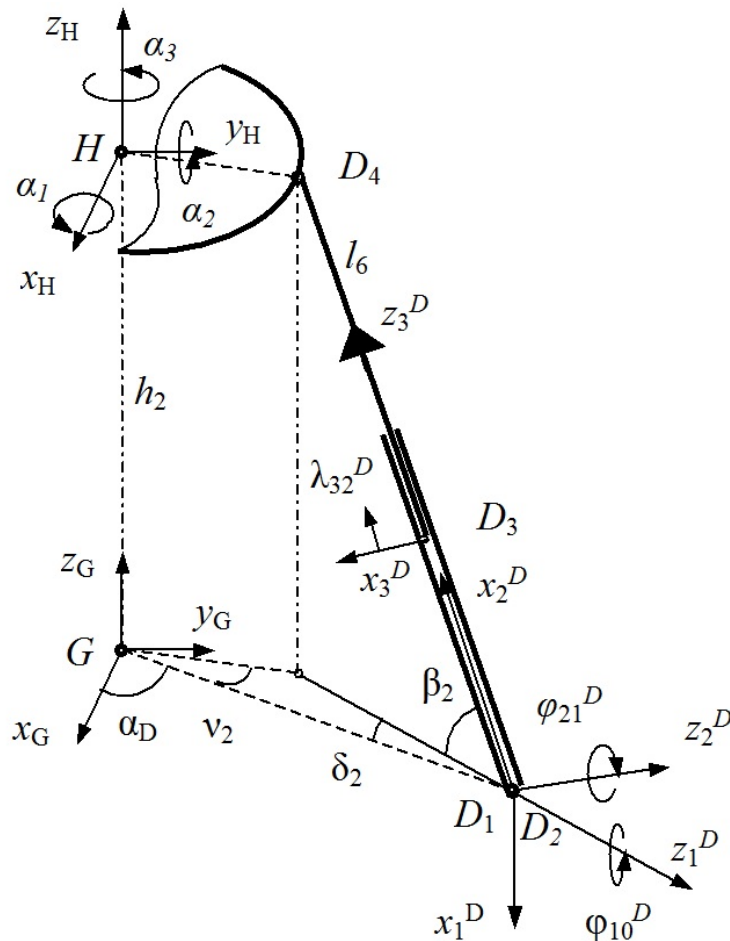


Fig. 4 –Kinematical scheme of first leg  $D$  of upper module.

Moreover, all legs are extended at equal lengths, starting from the same initial position  $l_4$ , and the angles of orientation of universal joints and spherical joints are given by following relations

$$\alpha_D = 0, \quad \alpha_E = -\alpha_E = \frac{2\pi}{3}, \quad \nu_2 = \frac{\pi}{3}, \quad \delta_2 = -\frac{\pi}{3},$$

$$h_2 = R_2 \operatorname{tg} \beta_2 = (l_4 + l_6) \sin \beta_2. \quad (2)$$

Starting from the origins  $O, G$  and pursuing along six independent legs  $OA_1A_2A_3A_4$ ,  $OB_1B_2B_3B_4$ ,  $OC_1C_2C_3C_4$ ,  $GD_1D_2D_3D_4$ ,  $GE_1E_2E_3E_4$ ,  $GF_1F_2F_3F_4$ , we obtain following matrices of transformation

$$p_{10} = p_{10}^{\varphi} a_1^{\delta} \theta_4 a_{\alpha}^i, \quad p_{21} = p_{21}^{\varphi} a_1^{\beta} \theta_1^T, \quad p_{32} = \theta_2, \quad p_{20} = p_{21} p_{10}, \quad p_{30} = p_{32} p_{20}$$

$$(p = a, b, c), \quad (i = A, B, C)$$

$$q_{10} = q_{10}^{\varphi} \theta_2 a_2^{\delta} a_{\alpha}^j, \quad q_{21} = q_{21}^{\varphi} a_2^{\beta} \theta_2 \theta_3, \quad q_{32} = \theta_2, \quad q_{20} = q_{21} q_{10}, \quad q_{30} = q_{32} q_{20}$$

$$(q = d, e, f) \quad (j = D, E, F), \quad (3)$$

where we denote the matrices [13]:

$$p_{\tau, \tau-1}^{\varphi} = \operatorname{rot}(z, \varphi_{\tau, \tau-1}^i), \quad q_{k, k-1}^{\varphi} = \operatorname{rot}(z, \varphi_{\tau, \tau-1}^j) \quad (\tau = 1, 2)$$

$$a_{\alpha}^i = \operatorname{rot}(z, \alpha_i), \quad a_{\alpha}^j = \operatorname{rot}(z, \alpha_j),$$

$$a_{\sigma}^{\delta} = \operatorname{rot}(z, \delta_{\sigma}), \quad a_{\sigma}^{\beta} = \operatorname{rot}(z, \beta_{\sigma}), \quad a_{\sigma}^{\nu} = \operatorname{rot}(z, \nu_{\sigma}) \quad (\sigma = 1, 2)$$

$$\theta_1 = \operatorname{rot}(x, \pi/2), \quad \theta_2 = \operatorname{rot}(y, \pi/2), \quad \theta_3 = \operatorname{rot}(z, \pi/2), \quad \theta_4 = \operatorname{rot}(y, \pi). \quad (4)$$

In a forward geometric problem, it can be considered that the coordinates  $x_0^G, y_0^G, z_0^G$  of mass center of lower moving platform and others six Euler angles  $\alpha_1, \alpha_2, \alpha_3$ , characterizing the sequence of orthogonal concurrent rotations around its centre  $H$  of upper moving platform, give completely the position of serial-parallel hybrid mechanism. Since all rotations take place successively about three moving coordinate axes, the general rotation matrix  $h_{30} = h_{32} h_{21} h_{10}$  of second moving platform is obtained by multiplying some relative basic matrices

$$h_{10} = a_1^{\alpha} \theta_2, \quad h_{21} = a_2^{\alpha} \theta_2 \theta_3, \quad h_{32} = a_3^{\alpha} \theta_3 \theta_2 \theta_3, \quad (5)$$

where  $a_l^{\alpha} = \operatorname{rot}(z, \alpha_l)$ ,  $l = 1, 2, 3$ .

Consider, for example, that during three seconds the coordinates of the center  $G$  and the angles of orientation  $\alpha_l$  can describe the instantaneous relative motions of the platforms through following analytical functions

$$\frac{x_0^G}{x_0^{G*}} = \frac{y_0^G}{y_0^{G*}} = \frac{h_1 - z_0^G}{z_0^{G*}} = \frac{\alpha_l}{\alpha_l^*} = 1 - \cos \frac{\pi}{3} t, \quad (6)$$

where the values  $2x_0^{G*}, 2y_0^{G*}, 2z_0^{G*}, 2\alpha_l^*$ , denote the final positions of the moving platforms.

A set of 18 independent variables  $\varphi_{\tau, \tau-1}^i, \lambda_{32}^i, \varphi_{\tau, \tau-1}^j, \lambda_{32}^j$ , characterizing the kinematics of two modules, will be determined through 18 scalar equations, which are easily generated by some vector-loop constraint conditions

$$\begin{aligned} \vec{r}_{10}^i + \sum_{k=1}^3 p_{k0}^T \vec{r}_{k+1,k}^i - \vec{r}_G^i &= \vec{r}_0^G \\ \vec{r}_{10}^j + \sum_{k=1}^3 q_{k0}^T \vec{r}_{k+1,k}^j - h_{30}^T \vec{r}_H^j &= \vec{r}_G^H, \end{aligned} \quad (7)$$

where

$$\begin{aligned} \vec{r}_{10}^i &= R_1 a_\alpha^{iT} \vec{u}_1, \quad \vec{r}_{21}^i = \vec{0}, \quad \vec{r}_{32}^i = (l_1 + \lambda_{32}^i) \vec{u}_1, \quad \vec{r}_{43}^i = l_3 \vec{u}_3 \\ \vec{r}_{10}^j &= R_2 a_\alpha^{jT} \vec{u}_1, \quad \vec{r}_{21}^j = \vec{0}, \quad \vec{r}_{32}^j = (l_4 + \lambda_{32}^j) \vec{u}_1, \quad \vec{r}_{43}^j = l_6 \vec{u}_3 \\ \vec{r}_G^i &= r_1 a_\alpha^{iT} a_1^{vT} \vec{u}_1, \quad \vec{r}_H^j = r_2 a_\alpha^{jT} a_2^{vT} \vec{u}_1, \quad \vec{r}_0^G = [x_0^G \ y_0^G \ z_0^G]^T, \quad \vec{r}_G^H = h_2 \vec{u}_3, \\ \vec{u}_1 &= [1 \ 0 \ 0]^T, \quad \vec{u}_2 = [0 \ 1 \ 0]^T, \quad \vec{u}_3 = [0 \ 0 \ 1]^T. \end{aligned} \quad (8)$$

From the vector equations (7) we obtain an inverse geometric solution for the spatial hybrid robot:

$$\begin{aligned} (l_1 + l_3 + \lambda_{32}^i) \sin(\varphi_{10}^i + \delta_1) \cos(\varphi_{21}^i + \beta_1) &= r_1 \sin \nu_1 - x_0^G \sin \alpha_i + y_0^G \cos \alpha_i - \\ -(l_1 + l_3 + \lambda_{32}^i) \sin(\varphi_{10}^i + \delta_1) \cos(\varphi_{21}^i + \beta_1) &= r_1 \cos \nu_1 + x_0^G \cos \alpha_i + y_0^G \sin \alpha_i - R_1 \\ (l_1 + l_3 + \lambda_{32}^i) \sin(\varphi_{21}^i + \beta_1) &= z_0^G \\ (l_4 + l_6 + \lambda_{32}^j) \cos(\varphi_{21}^j + \beta_2) &= R_2 \cos \delta_2 - \vec{u}_1^T \{ \vec{r}_G^H + h_{30}^T \vec{r}_H^j \} \cos(\alpha_j + \delta_2) - \\ &\quad - \vec{u}_2^T \{ \vec{r}_G^H + h_{30}^T \vec{r}_H^j \} \sin(\alpha_j + \delta_2) \\ (l_4 + l_6 + \lambda_{32}^j) \sin \varphi_{10}^j \sin(\varphi_{21}^j + \beta_2) &= -R_2 \sin \delta_2 + \vec{u}_1^T \{ \vec{r}_G^H + h_{30}^T \vec{r}_H^j \} \sin(\alpha_j + \delta_2) - \\ &\quad - \vec{u}_2^T \{ \vec{r}_G^H + h_{30}^T \vec{r}_H^j \} \cos(\alpha_j + \delta_2) \\ (l_4 + l_6 + \lambda_{32}^j) \cos \varphi_{10}^j \sin(\varphi_{21}^j + \beta_2) &= \vec{u}_3^T \{ \vec{r}_G^H + h_{30}^T \vec{r}_H^j \} \end{aligned} \quad (9)$$



The motion of the compounding elements of the hybrid robot are characterized by following relative velocities of joints and relative angular velocities

$$\begin{aligned} \vec{v}_{\tau,\tau-1}^i &= \vec{0}, \quad \vec{v}_{\tau,\tau-1}^j = \vec{0}, \quad \vec{v}_{32}^i = \dot{\lambda}_{32}^i \vec{u}_3, \quad \vec{v}_{32}^j = \dot{\lambda}_{32}^j \vec{u}_3, \\ \vec{\omega}_{\tau,\tau-1}^i &= \dot{\phi}_{\tau,\tau-1}^i \vec{u}_3, \quad \vec{\omega}_{\tau,\tau-1}^j = \dot{\phi}_{\tau,\tau-1}^j \vec{u}_3, \quad \vec{\omega}_{32}^i = \vec{0}, \quad \vec{\omega}_{32}^j = \vec{0} \quad (\tau=1, 2). \end{aligned} \quad (10)$$

To describe the absolute kinematical state of each link of leg A, for example, we compute the linear velocity  $\vec{v}_{k0}^A$ , the angular velocity  $\vec{\omega}_{k0}^A$  and the *associate skew-symmetric matrix*  $\tilde{\omega}_{k0}^A$  in terms of the vectors of the preceding body, using a recursive manner:

$$\begin{aligned} \vec{v}_{k0}^A &= a_{k,k-1} \vec{v}_{k-1,0}^A + a_{k,k-1} \tilde{\omega}_{k-1,0}^A \vec{r}_{k,k-1}^A + v_{k,k-1}^A \vec{u}_3, \\ \vec{\omega}_{k0}^A &= a_{k,k-1} \vec{\omega}_{k-1,0}^A + \omega_{k,k-1}^A \vec{u}_3, \quad \tilde{\omega}_{k0}^A = a_{k,k-1} \tilde{\omega}_{k-1,0}^A a_{k,k-1}^T + \omega_{k,k-1}^A \tilde{u}_3. \end{aligned} \quad (11)$$

Starting from the derivatives of geometrical constraints (7) and using the skew-symmetric matrix

$$\tilde{\omega}_{30} = h_{30} \dot{h}_{30}^T = \dot{\alpha}_1 h_{32} h_{21} \tilde{u}_3 h_{21}^T h_{32}^T + \dot{\alpha}_2 h_{32} \tilde{u}_3 h_{32}^T + \dot{\alpha}_3 \tilde{u}_3, \quad (12)$$

associated to the angular velocity  $\vec{\omega}_{30} = \dot{\alpha}_1 h_{32} h_{21} \vec{u}_3 + \dot{\alpha}_2 h_{32} \vec{u}_2 + \dot{\alpha}_3 \vec{u}_3$  of upper moving platform, we obtain the *matrix conditions of connectivity* [14]:

$$\vec{V}_i = [N_i]^{-1} \vec{P}_i, \quad \vec{V}_j = [N_j]^{-1} \vec{P}_j, \quad (13)$$

where following terms determines the contents of  $3 \times 3$  invertible square matrices  $[N_i], [N_j]$  and the column matrices  $\vec{P}_i, \vec{P}_j$ :

$$\begin{aligned} n_{m1}^i &= u_m^T p_{10}^T \tilde{u}_3 p_{21}^T \vec{r}_{42}^i, \quad n_{m2}^i = \vec{u}_m^T p_{20}^T \tilde{u}_3 \vec{r}_{42}^i, \quad n_{m3}^i = \vec{u}_m^T p_{20}^T \vec{u}_1, \quad \vec{r}_{42}^i = \vec{r}_{32}^i + p_{32}^T \vec{r}_{43}^i, \\ n_{m1}^j &= u_m^T q_{10}^T \tilde{u}_3 q_{21}^T \vec{r}_{42}^j, \quad n_{m2}^j = \vec{u}_m^T q_{20}^T \tilde{u}_3 \vec{r}_{42}^j, \quad n_{m3}^j = \vec{u}_m^T q_{20}^T \vec{u}_1, \quad \vec{r}_{42}^j = \vec{r}_{32}^j + p_{32}^T \vec{r}_{43}^j, \\ p_m^i &= \vec{u}_m^T \vec{r}_0^i, \quad p_m^j = \vec{u}_m^T h_{30}^T \tilde{\omega}_{30} \vec{r}_H^j \quad (m=1, 2, 3). \end{aligned} \quad (14)$$

Finally, the relative velocities  $\vec{V}_i = [\omega_{10}^i \quad \omega_{21}^i \quad v_{32}^i]^T$ ,  $\vec{V}_j = [\omega_{10}^j \quad \omega_{21}^j \quad v_{32}^j]^T$  are obtained from above equations (13).

Based on another conditions of connectivity, expressions of relative accelerations  $\vec{\Gamma}_i = [\varepsilon_{10}^i \quad \varepsilon_{21}^i \quad \gamma_{32}^i]^T$ ,  $\vec{\Gamma}_j = [\varepsilon_{10}^j \quad \varepsilon_{21}^j \quad \gamma_{32}^j]^T$  are obtained from the column matrix

$$\vec{\Gamma}_i = [N_i]^{-1} \vec{S}_i, \quad \vec{\Gamma}_j = [N_j]^{-1} \vec{S}_j, \quad (15)$$

where following terms determine the contents of column matrices  $\vec{S}_i = \dot{\vec{P}}_i - [\dot{N}_i]\vec{V}_i$ ,  $\vec{S}_j = \dot{\vec{P}}_j - [\dot{N}_j]\vec{V}_j$ :

$$\begin{aligned}
s_m^i &= \vec{u}_m^T \ddot{\vec{r}}_0^G - \omega_{10}^i \omega_{10}^i \vec{u}_m^T p_{10}^T \tilde{u}_3 \tilde{u}_3 p_{21}^T \vec{r}_{42}^i - \omega_{21}^i \omega_{21}^i \vec{u}_m^T p_{20}^T \tilde{u}_3 \tilde{u}_3 \vec{r}_{42}^i - \\
&- 2\omega_{10}^i \omega_{21}^i \vec{u}_m^T p_{10}^T \tilde{u}_3 p_{21}^T \tilde{u}_3 \vec{r}_{42}^i - 2\omega_{10}^i v_{32}^i \vec{u}_j^T p_{10}^T \tilde{u}_3 p_{21}^T \vec{u}_1 - 2\omega_{21}^i v_{32}^i \vec{u}_m^T p_{20}^T \tilde{u}_3 \vec{u}_1 \\
s_m^j &= \vec{u}_m^T q_{30}^T \{\tilde{\omega}_{30} \tilde{\omega}_{30} + \tilde{\varepsilon}_{30}\} \vec{r}_H^j - \omega_{10}^j \omega_{10}^j \vec{u}_l^T q_{10}^T \tilde{u}_3 \tilde{u}_3 q_{21}^T \vec{r}_{42}^j - \omega_{21}^j \omega_{21}^j \vec{u}_l^T q_{20}^T \tilde{u}_3 \tilde{u}_3 \vec{r}_{42}^j - \\
&- 2\omega_{10}^j \omega_{21}^j \vec{u}_m^T q_{10}^T \tilde{u}_3 q_{21}^T \tilde{u}_3 \vec{r}_{42}^j - 2\omega_{10}^j v_{32}^j \vec{u}_m^T q_{10}^T \tilde{u}_3 q_{21}^T \vec{u}_1 - 2\omega_{21}^j v_{32}^j \vec{u}_m^T q_{20}^T \tilde{u}_3 \vec{u}_1 \quad (16) \\
\tilde{\omega}_{30} \tilde{\omega}_{30} + \tilde{\varepsilon}_{30} &= \ddot{\alpha}_1 h_{32} h_{21} \tilde{u}_3 h_{21}^T h_{32}^T + \ddot{\alpha}_2 h_{32} \tilde{u}_3 h_{32}^T + \ddot{\alpha}_3 \tilde{u}_3 + \dot{\alpha}_1^2 h_{32} h_{21} \tilde{u}_3 \tilde{u}_3 h_{21}^T h_{32}^T + \\
&+ \dot{\alpha}_2^2 h_{32} \tilde{u}_3 \tilde{u}_3 h_{32}^T + \dot{\alpha}_3^2 \tilde{u}_3 \tilde{u}_3 + 2\dot{\alpha}_1 \dot{\alpha}_2 h_{32} h_{21} \tilde{u}_3 h_{21}^T \tilde{u}_3 h_{32}^T + \\
&+ 2\dot{\alpha}_2 \dot{\alpha}_3 h_{32} \tilde{u}_3 h_{32}^T \tilde{u}_3 + 2\dot{\alpha}_3 \dot{\alpha}_1 h_{32} h_{21} \tilde{u}_3 h_{21}^T h_{32}^T \tilde{u}_3.
\end{aligned}$$

Following relations give the linear accelerations  $\vec{\gamma}_{k0}^A$ , the angular accelerations  $\vec{\varepsilon}_{k0}^A$  and the *significant matrices*  $\tilde{\omega}_{k0}^A \tilde{\omega}_{k0}^A + \tilde{\varepsilon}_{k0}^A$  of each link from the leg A, for example:

$$\begin{aligned}
\vec{\gamma}_{k0}^A &= a_{k,k-1} \vec{\gamma}_{k-1,0}^A + a_{k,k-1} \{\tilde{\omega}_{k-1,0}^A \tilde{\omega}_{k-1,0}^A + \tilde{\varepsilon}_{k-1,0}^A\} \vec{r}_{k,k-1}^A + \\
&+ 2v_{k,k-1}^A a_{k,k-1} \tilde{\omega}_{k-1,0}^A a_{k,k-1}^T \vec{u}_3 + \gamma_{k,k-1}^A \vec{u}_3 \\
\vec{\varepsilon}_{k0}^A &= a_{k,k-1} \vec{\varepsilon}_{k-1,0}^A + \varepsilon_{k,k-1}^A \vec{u}_3 + \omega_{k,k-1}^A a_{k,k-1} \tilde{\omega}_{k-1,0}^A a_{k,k-1}^T \vec{u}_3 \quad (17) \\
\tilde{\omega}_{k0}^A \tilde{\omega}_{k0}^A + \tilde{\varepsilon}_{k0}^A &= a_{k,k-1} \{\tilde{\omega}_{k-1,0}^A \tilde{\omega}_{k-1,0}^A + \tilde{\varepsilon}_{k-1,0}^A\} a_{k,k-1}^T + \\
&+ \omega_{k,k-1}^A \omega_{k,k-1}^A \tilde{u}_3 \tilde{u}_3 + \varepsilon_{k,k-1}^A \tilde{u}_3 + 2\omega_{k,k-1}^A a_{k,k-1} \tilde{\omega}_{k-1,0}^A a_{k,k-1}^T \tilde{u}_3.
\end{aligned}$$

As application let us consider a serial-parallel hybrid mechanism which has following mechanical and architectural characteristics

$$x_0^{G*} = 0.05 \text{ m}, \quad y_0^{G*} = 0.05 \text{ m}, \quad z_0^{G*} = 0.15 \text{ m}$$

$$\alpha_1^* = \frac{\pi}{12}, \quad \alpha_2^* = \frac{\pi}{18}, \quad \alpha_3^* = \frac{\pi}{36}, \quad \Delta t = 3 \text{ s}$$

$$R_1 = 3r_1 = l_3 = 0.6 \text{ m}, \quad h_1 = 0.8 \text{ m}, \quad l = 0.75 \text{ m}, \quad r_2 = R_2 = l/\sqrt{3}, \quad l_4 = 0.25 \text{ m}, \\ l_6 = 1.25 \text{ m}.$$

Using MATLAB software, a computer program was used to solve the kinematics of the hybrid parallel robot. To develop the algorithm, it is assumed that the mechanism starts at rest from a central configuration.

As example, we consider that the lower platform moves along a *rectilinear horizontal trajectory* without any rotation, while the upper platform rotates about  $x_H$  horizontal axis with a variable angular acceleration  $\ddot{\alpha}_1$ .

The time-history for the input displacements  $\lambda_{32}^i$  (Fig.5),  $\lambda_{32}^j$  (Fig.6), relative velocities  $v_{32}^i$  (Fig.7),  $v_{32}^j$  (Fig.8) and relative accelerations  $\gamma_{32}^i$  (Fig.9),  $\gamma_{32}^j$  (Fig.10) is computed for a period of  $\Delta t = 3$  seconds in terms of given above analytical equations (6).

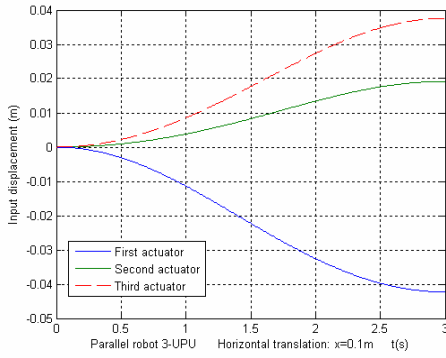


Fig. 5 – Lower module: input displacements  $\lambda_{32}^i$ .

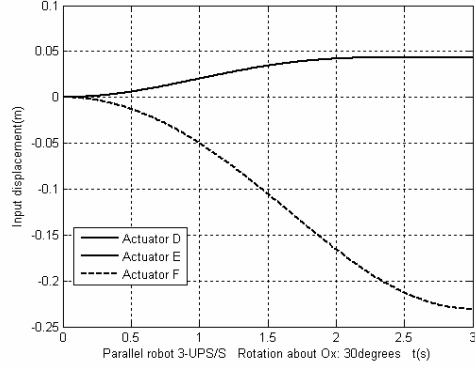


Fig. 6 – Upper module: input displacements  $\lambda_{32}^j$ .

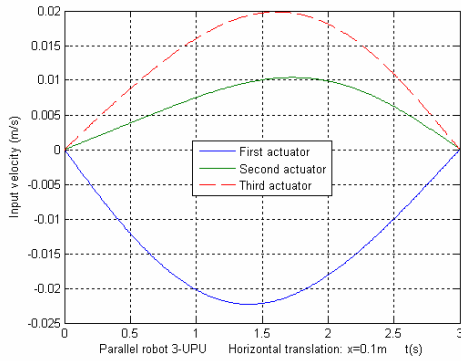


Fig. 7 – Lower module: input velocities  $v_{32}^i$ .

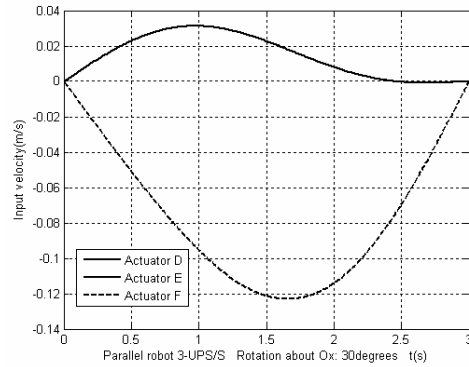


Fig. 8 – Upper module: input velocities  $v_{32}^j$ .

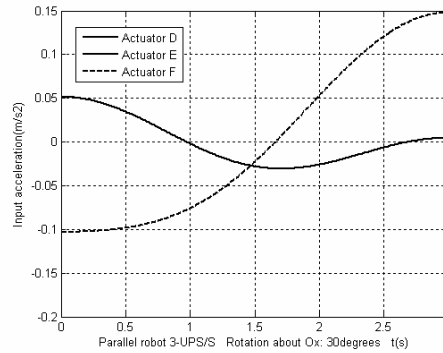
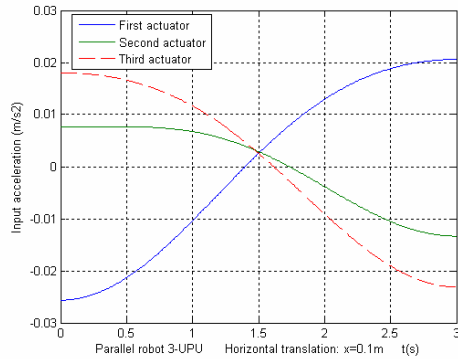


Fig. 9 – Lower module: input accelerations  $\gamma_{32}^i$ . Fig. 10 – Upper module: input accelerations  $\gamma_{32}^j$ .

Due to the relative rotation of upper moving platform, we notice that the distribution of displacement, velocity and acceleration depicted in Figs. 6, 8, 10 is the same, at any instant, for two of three actuators of upper module.

The simulation through the program certifies that some of the major advantages of the current matrix recursive formulation are accuracy and a smaller processing time of numerical computation.

#### 4. CONCLUSIONS

Some exact relations that give in real-time the position, velocity and acceleration of each element of a two-module hybrid parallel robot have been established in the present paper. Choosing the appropriate serial kinematical circuits connecting many moving platforms, the present concept and the procedure above developed can be immediately extended to analysis of a complex robotic system composed of a multitude serially arranged similar parallel modules, but are also applicable to study of hybrid robots that are composed of different structures of parallel modules, where the number of links of the mechanisms is increased and the value of total degrees-of-freedom is augmented.

*Received on November 19, 2015*

#### REFERENCES

1. TSAI, L-W., *Robot analysis: the mechanics of serial and parallel manipulators*, Wiley, 1999.
2. PLITEA, N., LESE, D., PISLA, D., VAIDA, C., *Structural design and kinematics of a new parallel reconfigurable robot*, *Robotics and Computer-Integrated Manufacturing*, **29**, 1, pp. 219–235, 2013.
3. MERLET, J-P., *Parallel robots*, Kluwer Academic, 2000.

4. GOGU, G., *T2R1-type parallel manipulators with bifurcated planar-spatial motion*, European Journal of Mechanics, A/Solids, **33**, pp. 1–11, 2012.
5. TSAI, L-W., JOSHI, S., *Kinematics analysis of 3-DOF position mechanisms for use in hybrid kinematic machines*, ASME Journal of Mechanical Design, **124**, 2, pp. 245–253, 2002.
6. TANEV, T.K., *Kinematics of a hybrid (parallel–serial) robot manipulator*, Mechanism and Machine Theory, **35**, 9, pp. 1183–1196, 2000.
7. IBRAHIM, O., KHALIL, W., *Inverse and direct dynamic models of hybrid robots*, Mechanism and Machine Theory, **45**, 4, pp. 627–640, 2000.
8. CAMPOS, A., BUDDE, C., HESSELBACH, J., *A type synthesis method for hybrid robot structures*, Mechanism and Machine Theory, **43**, 8, pp. 984–995, 2008.
9. LIU, N., WU, J., *Kinematics and Application of a Hybrid Industrial Robot – Delta-RST*, Sensors & Transducers, **169**, 4, pp. 186–192, 2014.
10. SHAHINPOOR, M., *Kinematics of a parallel-serial (hybrid) manipulator*, Journal of Robotic Systems, **9**, 1, pp. 17–36, 1992.
11. CHENG, H.H., LEE, J.J., PENKAR, R., *Kinematic analysis of a hybrid serial-and-parallel-driven redundant industrial manipulator*, International Journal of Robotics and Automation, **10**, 4, pp. 159–166, 1995.
12. GALLARDO, J., LESSO, R., RICO, J.M., ALICI, G., *The kinematics of modular spatial hyper-redundant manipulators formed from RPS type limbs*, Robotics and Autonomous Systems, **59**, 1, pp. 12–21, 2011.
13. STAICU, S., *Matrix modeling of inverse dynamics of spatial and planar parallel robots*, Multibody System Dynamics, **27**, 2, pp. 239–265, 2012.
14. LI, Y., STAICU, S., *Inverse dynamics of a 3-PRC parallel kinematic machine*, Nonlinear Dynamics, **67**, 2, pp. 1031–1041, 2012.